



ARTICLE

Three macrophage subsets are identified in the uterus during early human pregnancy

Xiangxiang Jiang^{1,2}, Mei-Rong Du³, Min Li⁴ and Hongmei Wang¹

Macrophages are crucial for a successful pregnancy, and malfunctions of decidual macrophages correlate with adverse pregnancy outcomes, such as spontaneous abortion and preeclampsia. Previously, decidual macrophages were often thought to be a single population. In the present study, we identified three decidual macrophage subsets, CCR2–CD11c^{LO} (CD11c^{low}, ~80%), CCR2–CD11c^{HI} (CD11c^{high}, ~5%), and CCR2+CD11c^{HI} (CD11c^{high}, 10–15%), during the first trimester of human pregnancy by flow cytometry analysis. CCR2–CD11c^{LO} macrophages are widely distributed in the decidua, while CCR2–CD11c^{HI} and CCR2+CD11c^{HI} macrophages are primarily detected close to extravillous trophoblast cells according to immunofluorescence staining. According to RNA sequencing bioinformatics analysis and in vitro functional studies, these three subsets of macrophages have different phagocytic capacities. CCR2+CD11c^{HI} macrophages have pro-inflammatory characteristics, while the CCR2–CD11c^{HI} population is suggested to be anti-oxidative and anti-inflammatory due to its high expression of critical heme metabolism-related genes, suggesting that these two subsets of macrophages maintain an inflammatory balance at the leading edge of trophoblast invasion to facilitate the clearance of pathogen infection as well as maintain the homeostasis of the maternal-fetal interface. The present study physiologically identifies three decidual macrophage subsets. Further clarification of the functions of these subsets will improve our understanding of maternal-fetal crosstalk in the maintenance of a healthy pregnancy.

Keywords: CCR2; CD11c; decidual macrophage subsets; extravillous trophoblast cells; inflammatory balance

Cellular & Molecular Immunology (2018) 15:1027–1037; <https://doi.org/10.1038/s41423-018-0008-0>

INTRODUCTION

During early human pregnancy, extravillous trophoblast cells (EVTs) migrate from the placental chorion villous column into the decidua and contact decidual immune cells, which are mainly composed of decidual natural killer (NK) cells, macrophages, and T cells.¹ Decidual NK cells, the most abundant (50–70%) leucocytes in the decidua, have been suggested to promote decidual vascular remodeling and fetal development.^{2–4} The function of decidual T cells (10–20%) is poorly defined, but regulatory T cells have been suggested to be involved in maternal-fetal tolerance.⁵ Decidual macrophages are the second most abundant leucocytes (10–20%) in the decidua,¹ and they have been suggested to promote vascular remodeling,^{1,6} the clearance of cell debris,^{7,8} and parturition.^{9,10} Macrophage depletion after conception has been reported to cause embryo implantation arrest,¹¹ highlighting the significance of macrophages during pregnancy. Macrophages are generally considered to have two populations, in vitro interferon gamma (IFN- γ), lipopolysaccharide (LPS)-induced pro-inflammatory M1 macrophages, and interleukin-4 (IL4)-induced anti-inflammatory M2 macrophages.¹² Decidual macrophages are usually considered to be M2 macrophages.^{1,13} However, studies also report that M1 macrophages play crucial roles in implantation and parturition.^{9,14,15} It seems that decidual macrophages maintain the phenotypic balance between pro-inflammatory M1 and

anti-inflammatory M2 macrophages during pregnancy.¹⁵ M1/M2 imbalance correlates with pathological pregnancies,^{15,16} such as preeclampsia,¹⁷ spontaneous abortion,¹⁸ and preterm labor.^{19,20} Although decidual macrophages may have M1 and M2 subtypes, M1 and M2 are, after all, in vitro concepts.¹² Under physiological conditions, whether decidual macrophages also have subsets deserves further investigation.

In the decidua, both NK cells and T cells have subsets. The identification of subsets has improved our understanding of the precise functions of these cells during pregnancy. Four different decidual NK cell subsets are characterized based on the expression of integrin alpha-M (CD11b) and CD27.²¹ CD11b–CD27– NK cells tend to be immature and have a potential for differentiation. CD11b–CD27+ and CD11b+CD27+ NK cells mainly secrete cytokines. CD11b+CD27– NK cells exhibit the highest cytolytic function. Decidual T cells mainly include CD4+ helper T (Th) cells and CD8+ cytotoxic T cells.^{1,22} Th1 and Th2 CD4+ T cells are found at the human maternal-fetal interface, and recurrent spontaneous abortion often correlates with an increased Th1/Th2 ratio.^{1,23} However, few studies have clearly identified decidual macrophage subsets.

In this study, utilizing a combination of C–C chemokine receptor type 2 (CCR2) and integrin alpha-X (CD11c), a molecule identified from a bioinformatics study,²⁴ we clearly separated human

¹State Key Laboratory of Stem Cell and Reproductive Biology, Institute of Zoology, Chinese Academy of Sciences, Beijing 100101, China; ²University of Chinese Academy of Sciences, Beijing 100049, China; ³Laboratory for Reproductive Immunology, Hospital of Obstetrics and Gynecology, Fudan University Shanghai Medical College, Shanghai 200011, China and ⁴Department of Obstetrics and Gynecology, Navy General Hospital of the Chinese PLA, Beijing 100048, China
Correspondence: Hongmei Wang (wanghm@ioz.ac.cn)

Received: 20 October 2017 Revised: 18 January 2018 Accepted: 18 January 2018

Published online: 4 April 2018

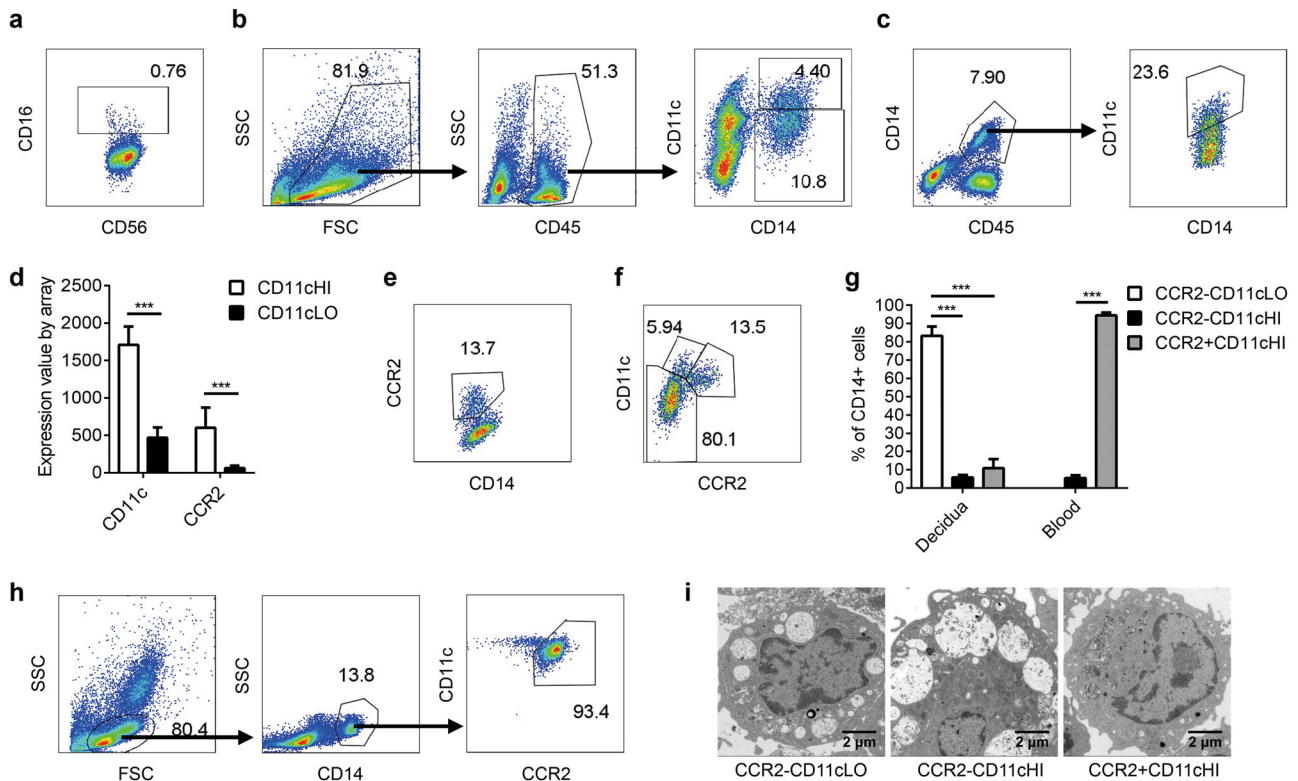


Fig. 1 Identification of three distinct subsets of macrophages at the maternal-fetal interface during the first trimester of human pregnancy. **a** Quality control of isolated primary decidual cells based on the low frequency of CD16⁺ NK cells. **b** Flow cytometry analysis of CD11c expression in CD45⁺ decidual immune cells. **c** Verification of two decidual macrophage subsets based on CD11c expression level. **d** Analysis of CCR2 expression in CD11cHI and CD11cLO macrophage subsets based on published microarray data. Expression matrix data were downloaded from the NCBI Gene Expression Omnibus under accession number GSE22342. Then, the expression values of CD11c (ITGAX) and CCR2 were copied to GraphPad, and multiple *t*-tests were performed to compare the differential expression of CD11c and CCR2 ($n = 8$, $***P < 0.001$). **e** Flow cytometry analysis of CCR2 expression in CD14⁺ decidual macrophages. **f** Flow cytometry analysis of CCR2 and CD11c expression in decidual macrophages. **g** The statistical percentages of the decidual macrophage subsets and peripheral monocyte subsets ($n = 6$, one-way ANOVA, $***P < 0.001$). **h** Flow cytometry analysis of CCR2 and CD11c expression in peripheral blood monocytes. **i** Representative TEM images of the three decidual macrophage subsets

decidual macrophages into three subsets (CCR2–CD11cLO, CCR2–CD11cHI, CCR2+CD11cHI). We then studied the localization of the three populations of macrophages according to immunofluorescence, the morphology of these cells as determined by flow cytometry analysis and transmission electron microscopy (TEM), and the function of these cells as determined by RNA sequencing (RNA-Seq) bioinformatics analysis and *in vitro* experiments.

MATERIALS AND METHODS

Human peripheral blood and decidua samples

Human peripheral blood (10 ml) and decidua (8–16 g) were anonymously collected from clinically normal first trimester (6–8 weeks) pregnant women (20–35 years old) who underwent elective termination of pregnancy for non-medical reasons. Informed consent was obtained from all women who donated their decidua and peripheral blood, and human decidua samples were collected in accordance with the policy of the Ethics Committee of Navy General Hospital of the Chinese PLA, Beijing, People's Republic of China. All samples were used according to standard experimental protocols approved by the Ethics Committee of the Institute of Zoology, Chinese Academy of Sciences.

Isolation of primary decidual cells

Primary decidual cells, comprising decidual stromal cells and decidual immune cells, were isolated as previously described^{25,26}

with modifications. Briefly, freshly collected decidua was rinsed several times with PBS until there were no obvious blood clots; then, the decidua was placed into a small bottle and cut into small pieces, which were digested with collagenase Type IV (0.5 mg/ml, C5138, Sigma-Aldrich, St. Louis, MO, USA) and DNase I (0.1 mg/ml, DN25, Sigma-Aldrich) for 45 min. The released decidual cells were filtered through 100, 200, and 400 mesh sieves. To exclude any remaining red blood cells, the filtered cells were lysed by red blood cell lysis buffer. Finally, the pelleted decidual cells were resuspended in PBS or full RPMI medium (SH30809.01, HyClone, Logan, UT, USA) with 10% FBS (10099–141, Gibco, Carlsbad, CA, USA), 100 units/ml penicillin and 100 μg/ml streptomycin. Cell viability was typically more than 90% as detected by an apoptosis assay kit (abs50001a, Absin, Shanghai, China). The low percentage (<2%) of peripheral NK cells (CD56+CD16+) in isolated primary decidual cells reflected little contamination by peripheral blood cells (Fig. 1a).

Flow cytometry analysis

Cells were incubated with Human TruStain FcX (422301, Biolegend, San Diego, CA, USA) for 30 min to block Fc receptors and subsequently stained with CD45-APC-cy7, CD14-BV421, CD11c-PE, and CCR2-APC for 30 min at 4°C. After three washes with PBS, approximately 50,000 cells were collected using a CytofLEX flow cytometer (Beckman Coulter, Brea, CA, USA), and the data were analyzed with FlowJo V10.2 (FlowJo, Ashland, OR, USA).

Isolation of three decidual macrophage subsets

First, decidual macrophages were enriched by CD14 magnetic beads (130-050-201, Miltenyi, Bergisch Gladbach, NRW, Germany) with magnetic-activated cell sorting (MACS). Next, three decidual macrophage subsets were purified by fluorescence-activated cell sorting (FACS) with a MoFlo XDP flow cytometer (Beckman Coulter) after labeling macrophages with CD14-FITC, CCR2-APC, and CD11c-PE. The purities of the sorted macrophage subsets were ~95% (Supplementary Figure S3).

Isolation of human peripheral monocytes

Peripheral blood mononuclear cells (PBMCs) were immediately isolated using the Ficoll-Hypaque (DKW-KLSH-0100, Dakewe, Shenzhen, GD, China) density gradient centrifugation method (15 min, 1500 × *g*) after fresh blood collection. CD14⁺ monocytes were purified from PBMCs by using CD14 magnetic beads.

RNA-Seq data analysis

Freshly sorted decidual macrophage subsets (>2 × 10⁵ cells) and peripheral monocytes (>2 × 10⁵ cells) were precipitated and lysed by TRIzol reagent (15596018, Ambion, Carlsbad, CA, USA) prior to transport to the Beijing Genomics Institute on dry ice. Total RNA was extracted using a phenol-chloroform method, and the quality of coordinate RNA samples was tested by an Agilent 2100. Next, 0.2 μg of total RNA from each sample was utilized to construct a sequencing library for Illumina HiSeq 4000 using a PE150 strategy. We obtained three groups, each including the three decidual macrophage subsets plus one peripheral monocyte population from early pregnancy. In total, 12 samples were sequenced. Raw data and processed data were uploaded to the NCBI Gene Expression Omnibus database under accession number GSE89323. We selected two better sequencing groups (eight samples) to analyze differentially expressed genes. Genes with low expression were excluded, and all 0 FPKM values were substituted as 0.01. We identified 3833 differentially expressed genes between these three decidual macrophage populations based on two fold differences from 12,392 filtered genes. Unsupervised heat map clustering analysis was performed by using Cluster 3.0.²⁷ The input data were first log-transformed, and we selected center genes using a median method. We then clustered the adjusted data on genes and arrays by using the average linkage method. The clustering results were visualized and exported by TreeView 1.1.6r4.²⁷ A principle component analysis (PCA) image was generated by R(3.3.3)/Bioconductor (3.4) with the “edgeR” and “limma” packages.²⁸ Kyoto encyclopedia of genes and genomes (KEGG)²⁹ and gene ontology – biological process (GO-BP)³⁰ enrichment analyses were executed by R/Bioconductor with the “clusterProfiler” package.³¹ A Venn diagram was constructed at <http://genevnn.sourceforge.net/>.³²

Isolation of decidual cells proximal or distal to EVT

We developed a method to isolate decidual cells proximal or distal to EVTs, which were positive for HLA class I histocompatibility antigen, alpha chain G (HLA-G).²⁵ Based on preliminary immunofluorescence staining experiments, the neat, less bloody and thick tissue that contained intact epidermal structures was decidual distal to EVTs, while the remaining bloody, anomalous small pieces of decidua were normally EVT-proximal decidua containing moderate EVTs.

Immunofluorescence staining

First trimester decidua was immediately fixed in 4% neutral paraformaldehyde (P6148, Sigma-Aldrich) overnight at 4 °C and subsequently embedded in paraffin. The tissue sections (5 μm) were dewaxed and rehydrated in xylene and ethanol gradients. Then, the slides were immersed in TE buffer (10 mM Tris, 1.0 mM EDTA, pH 9.0) and heated in a microwave oven at 92–98 °C for 15 min for antigen retrieval. After cooling to room temperature, the

sections were blocked with 10% goat serum for 30 min at room temperature before incubation with primary antibodies overnight at 4 °C, followed by incubation with Alexa Fluor-conjugated secondary antibodies for 1 h at room temperature. IgGs of the same species from which the primary antibody was generated were applied to negative control sections. The sections were subsequently counterstained with 4',6-diamidino-2-phenylindole (DAPI, D1306, Invitrogen, Carlsbad, CA, USA) and mounted with anti-fade mounting medium. Images were captured on a Carl Zeiss LSM 780 confocal laser-scanning microscope (Zeiss, Oberkochen, BW, Germany) and processed by ZEN 2012 (black edition) software. We examined the expression of critical genes, such as HMOX1, CCR2, and HLA-G, in samples from 60 normal pregnant women in the first trimester.

Western blot analysis

Decidual macrophage or peripheral monocyte proteins were extracted using SDS lysis buffer (2% SDS, 50 mM Tris-HCl pH 7.6, 2 mM EDTA and 10% glycerol). Proteins were quantified by using the BCA Protein Assay Kit (23227, Thermo Pierce, Waltham, MA, USA). Then, 5 μg of protein was subjected to SDS-PAGE gel electrophoresis and electrophoretically transferred onto a PVDF membrane. After blocking with 5% skim milk, the membrane was incubated with primary antibodies overnight at 4 °C. Then, the membrane was washed and incubated with corresponding horseradish peroxidase-conjugated secondary antibodies for 1 h at room temperature. The results were captured with a Gene Gnome Imaging System (Syngene, Cambridge, Cambs, UK). Beta-2-microglobulin (B2M) was used as the loading control. We performed at least six biological replicates for each protein blotted, and a representative result is shown.

Real-time PCR

Total RNA was extracted from decidual macrophage subsets using TRIzol reagent according to the manufacturer's instructions. Reverse transcription was performed with 0.2 μg of total RNA using SuperScript II Reverse Transcriptase (18064-014, Invitrogen) and an oligo-dT primer (Invitrogen). Real-time PCR was performed by using the SYBR II kit (RR820A, TaKaRa, Dalian, LN, China) according to the manufacturer's instructions on a Light Cycler 480 real-time PCR System (Roche, Basel, BS, Switzerland). The mRNA levels of the target genes were normalized to B2M, and relative expression was determined by the 2^{-ΔΔCt} method.

Antibodies and primers

The antibodies and primers used are listed in Supplementary Tables S1 and S2.

Enzyme-linked immunosorbent assay (ELISA)

Decidual macrophage subsets freshly isolated by MACS and FACS were seeded onto 48-well plates (10⁵ cells per well) with 0.2 ml of full RPMI medium in 5% CO₂ at 37 °C for 24 h. The supernatants of decidual macrophage subsets were collected by centrifugation and stored at -80 °C until ELISA assays were carried out. We performed ELISA according to the protocols of the ELISA kits to detect the secretory levels of interleukin-1 beta (IL-1B) (DKW12-1012-048, Dakewe) and prostaglandin E2 (PGE2) (KGE004B, R&D Systems, Minneapolis, MN, USA).

Transmission electron microscopy (TEM) experiment

Decidual macrophages (~5 × 10⁵ each) were fixed in 2.5% glutaraldehyde (A17876, Alfa Aesar, Heysham, Lancs, UK) in 0.1 M phosphate buffer (pH 7.4) for 2 h at room temperature. Then, the samples were sent to the Institute of Biophysics, Chinese Academy of Sciences for ultrathin sectioning. Ultrathin sections (70 nm) were further processed and captured under a Tecnai Spirit (120 kV) transmission electron microscope (FEI, Hillsboro, OR, USA).

Phagocytosis assay

Clostridium sordellii (C. sordellii, ATCC9714, China Center of Industrial Culture Collection, Beijing, China) was grown anaerobically in anaerobic medium (CM1513, Land Bridge, Beijing, China) at 37°C. A suspension of C. sordellii containing a bacterial concentration corresponding to 1×10^9 colony-forming units (CFU)/ml was collected. After two washes, C. sordellii cells were labeled with 5.0 µM carboxyfluorescein diacetate succinimidyl ester (CFSE, 65-0850-84, eBioscience, San Diego, CA, USA) for 40 min at 37°C.³³ A total of 5×10^5 decidual cells were incubated with 1×10^7 CFU CFSE-labeled C. sordellii in 24-well plates for 2 h at 37°C, or 1×10^5 decidual macrophages were incubated with 1×10^7 CFU C. sordellii. Next, decidual cells or macrophages were collected and incubated with Human TruStain FcX (422301, Biolegend) to block Fc receptors and subsequently stained with CD45-APC-cy7, CD14-BV421, CD11c-PE, and CCR2-APC for 30 min at 4°C. After three washes with PBS, the phagocytic capacity of decidual macrophages was determined by flow cytometry analysis. At least 50,000 cells were assayed, and the data were analyzed with FlowJo V10.2. Escherichia coli (E. coli, TOP10, Biomed, Beijing, China) was cultured in LB medium (Oxoid, Basingstoke, Hants, UK) under normoxia, and Listeria monocytogenes (L. monocytogenes, ATCC 19115, China General Microbiological Culture Collection Center, Beijing, China) was grown in brain heart infusion medium (CM1135, Oxoid) under normoxia. The subsequent processes were the same as those used for C. sordellii. When the phagocytosis efficiency of CCR2-CD11cLO macrophages was 20–40%, the assay was subjected to statistical analysis.

Statistical analysis

All experiments were repeated as indicated in the figure legends, and *n* indicates the number of independent biological repeats. We defined biological replicates starting from the processing of decidua and peripheral blood from different pregnant women. All statistical analyses were conducted with GraphPad Prism Version 7.0. Differences among groups were evaluated by using unpaired one-way analysis of variance (ANOVA) with correction by the Tukey method or multiple *t*-tests analysis with a false discovery rate approach corrected by the Benjamini, Krieger, and Yekutieli method. The data are presented as the mean \pm s.d. **P* < 0.05; ***P* < 0.01; ****P* < 0.001. For all statistical tests, *P* < 0.05 was considered statistically significant.

RESULTS

Identification of three distinct subsets of macrophages at the maternal-fetal interface during human first trimester pregnancy. A previous bioinformatics study reported that decidual macrophages could be divided into two subsets based on CD11c expression.²⁴ To confirm this observation, we freshly isolated decidual cells from human decidua at 6–8 weeks of gestation and subjected these cells to flow cytometry analysis using anti-CD14, CD45, and CD11c antibodies. The decidual macrophages were CD14+CD45+. Based on CD11c, decidual macrophages were clustered into two subsets (CD11cHI and CD11cLO) as expected (Fig. 1a–c). As not all of the CD11c-positive cells were macrophages (Fig. 1b), we needed to find a specific marker to localize these two subsets of macrophages. We examined all of the differentially expressed genes between these two macrophage subsets by analyzing the coordinate microarray data (GSE22342),²⁴ and fortunately, we found a chemokine receptor gene named CCR2 that was highly expressed in CD11cHI macrophages (Fig. 1d). CCR2 is the membranous receptor for C–C motif chemokine 2 (CCL2), and the CCR2–CCL2 signaling axis plays important roles in mediating monocyte migration and the progression of numerous inflammatory diseases.^{34–36} Using CCR2, we successfully divided decidual macrophages into two subsets (Fig. 1e). We initially

thought that CD11cHI macrophages were all positive for CCR2. However, when combined with CD11c, decidual macrophages were unexpectedly clustered into three subsets: CCR2-CD11cLO, CCR2-CD11cHI, and CCR2+CD11cHI (Fig. 1f). CCR2-CD11cLO macrophages were the most abundant macrophages (~80%), while CCR2-CD11cHI and CCR2+CD11cHI subsets accounted for ~5% and 5–15% of macrophages, respectively, at the maternal-fetal interface (Fig. 1f, g). Peripheral monocytes may serve as a source for tissue-resident macrophages,³⁷ such as decidual macrophages, so we then examined the expression levels of CCR2 and CD11c in monocytes. Most monocytes were CCR2+CD11cHI, and CD11c- and CD11cLO monocytes were barely detected (Fig. 1g, h).

After identifying three subsets of macrophages in the decidua during first trimester pregnancy, we next aimed to elucidate the morphology of these macrophage subsets. To this end, we purified these three macrophage subsets by FACS and cultured them for microscopy observation. CCR2-CD11cHI macrophages were significantly larger than the other two subsets (Supplementary Figure S1a). We also back-plotted the scatter graphs of these three macrophage populations during flow cytometry analysis, and we again found that CCR2-CD11cHI macrophages were the largest and had the largest variation in size and granularity (Supplementary Figure S1b). To further study the morphology of these subsets, we performed a TEM experiment. CCR2-CD11cHI decidual macrophages were the largest, with the most abundant and largest phagocytic vacuoles, while CCR2+CD11cHI decidual macrophages were the most compact, with only a few small phagocytic vacuoles (Fig. 1i). CCR2-CD11cLO macrophages were intermediately compact with some medium-size phagocytic vacuoles (Fig. 1i).

The localization of the three macrophage subsets at the maternal-fetal interface

To localize these three subsets of macrophages, specific markers were needed. CCR2+CD11cHI cells were able to be labeled by an anti-CCR2 antibody (Supplementary Figure S2a). However, markers to label CCR2-CD11cHI macrophages were lacking. To find markers, we purified the three subsets of decidual macrophages by combining MACS and FACS (Supplementary Figure S3) and performed a RNA-Seq experiment (GSE89323). Peripheral blood monocytes from early pregnant women were included as a control. We selected 485 specific genes (Supplementary Table S3) for CCR2-CD11cHI macrophages with two fold higher FPKM values than the other two subsets. Among these genes, secreted phosphoprotein 1 (SPP1) and heme oxygenase-1 (HMOX1) were among the most highly expressed genes in CCR2-CD11cHI cells (Fig. 2a), which was further verified by western blot analysis (Fig. 2b). By immunofluorescence staining on decidua sections of 6–8 weeks of gestation, we found that almost all HMOX1+ cells were CD14+ macrophages (Supplementary Figure S2b). Meanwhile, no overlapping signals between HMOX1 and CCR2 staining were observed (Supplementary Figure S2c). We thus selected HMOX1 to further distinguish the CCR2-CD11cHI and CCR2-CD11cLO macrophages. Meanwhile, the HMOX1 and SPP1 signals were almost overlapped (Supplementary Figure S2d), reflecting the accuracy of our method and results.

We performed immunofluorescence analysis with decidua paraffin sections from 60 pregnant women (6–8 weeks of gestation). CCR2-CD11cHI decidual macrophages (HMOX1+CD14+) were specifically localized close to HLA-G+EVTs (Fig. 2c). CCR2+CD11cHI decidual macrophages (CCR2+CD14+) were also mainly localized proximal to EVTJs (Fig. 2d), but were slightly further from and less strictly restrictive to EVTJs than the CCR2-CD11cHI subset. CCR2-CD11cLO cells (CD14+, CCR2-, and HMOX1-) were widespread in the decidua (Supplementary Figures S2a–c). To further confirm the spatial relationship between macrophage subsets and EVTJs, we enriched decidual cells

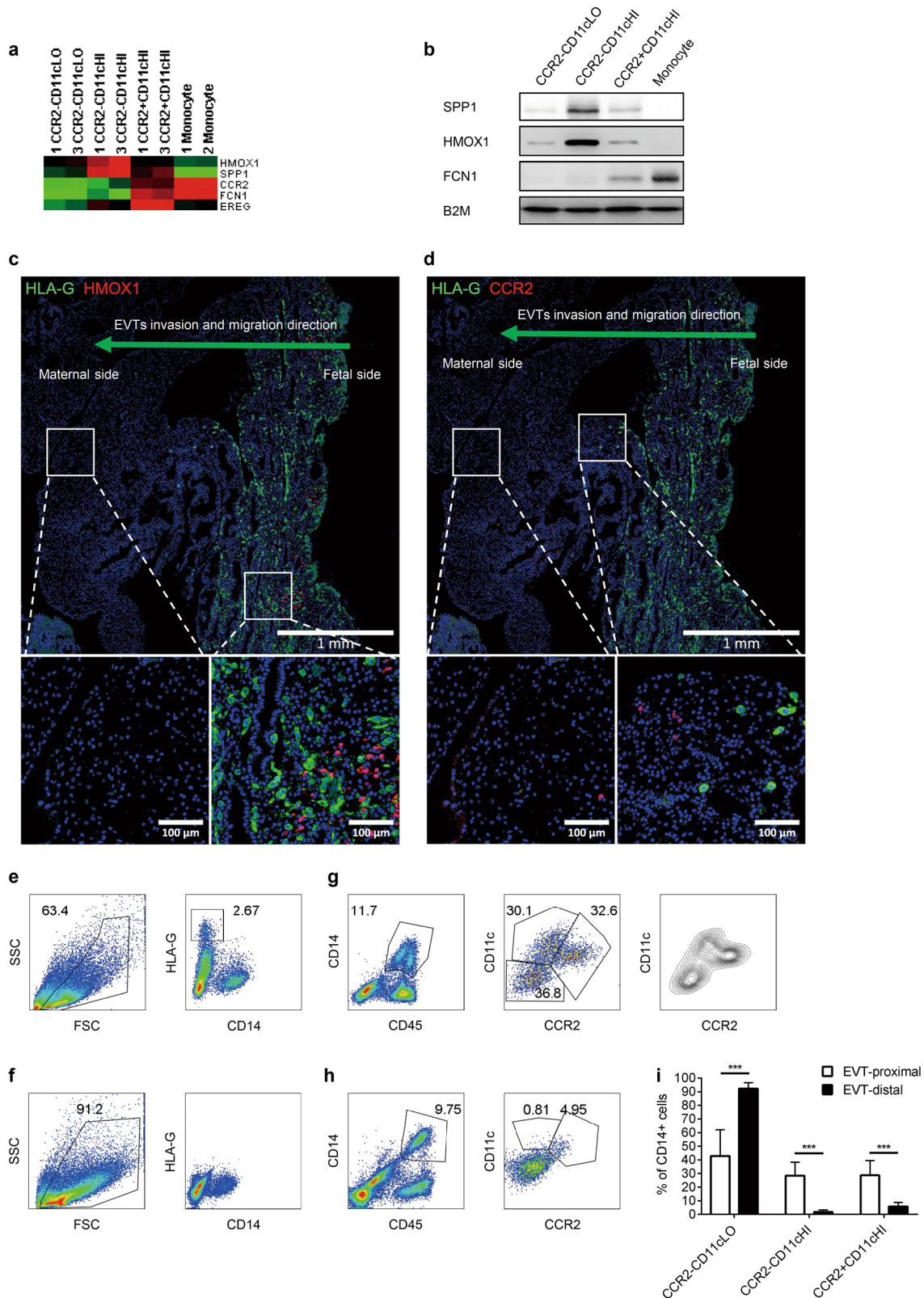


Fig. 2 Localization of the three macrophage subsets at the maternal–fetal interface. **a** Heat map showing highly expressed genes of two CD11cHI macrophage subsets. **b** Confirmation of highly expressed genes in two CD11cHI macrophage subsets based on western blot, with B2M as the loading control (here and after). **c** Representative immunofluorescence results for HLA-G and HMOX1 staining on decidual tissues from 7 weeks of gestation. **d** Representative immunofluorescence results for HLA-G and CCR2 staining on decidual tissues from 7 weeks of gestation. **e** Quality control for isolated primary decidual cells, which were proximal to EVTs, as indicated by HLA-G+ cells. **f** A lack of observation of HLA-G+ cells was used as the quality control for isolated primary decidual cells, which were distal to EVTs. **g** The percentages of the three decidual macrophage subsets derived from the decidua proximal to EVTs. **h** The percentages of the three decidual macrophage subsets derived from the decidua distal to EVTs. **i** The statistical percentages of the three decidual macrophage subsets derived from the decidua proximal or distal to EVTs ($n = 6$, multiple t -tests, $***P < 0.001$)

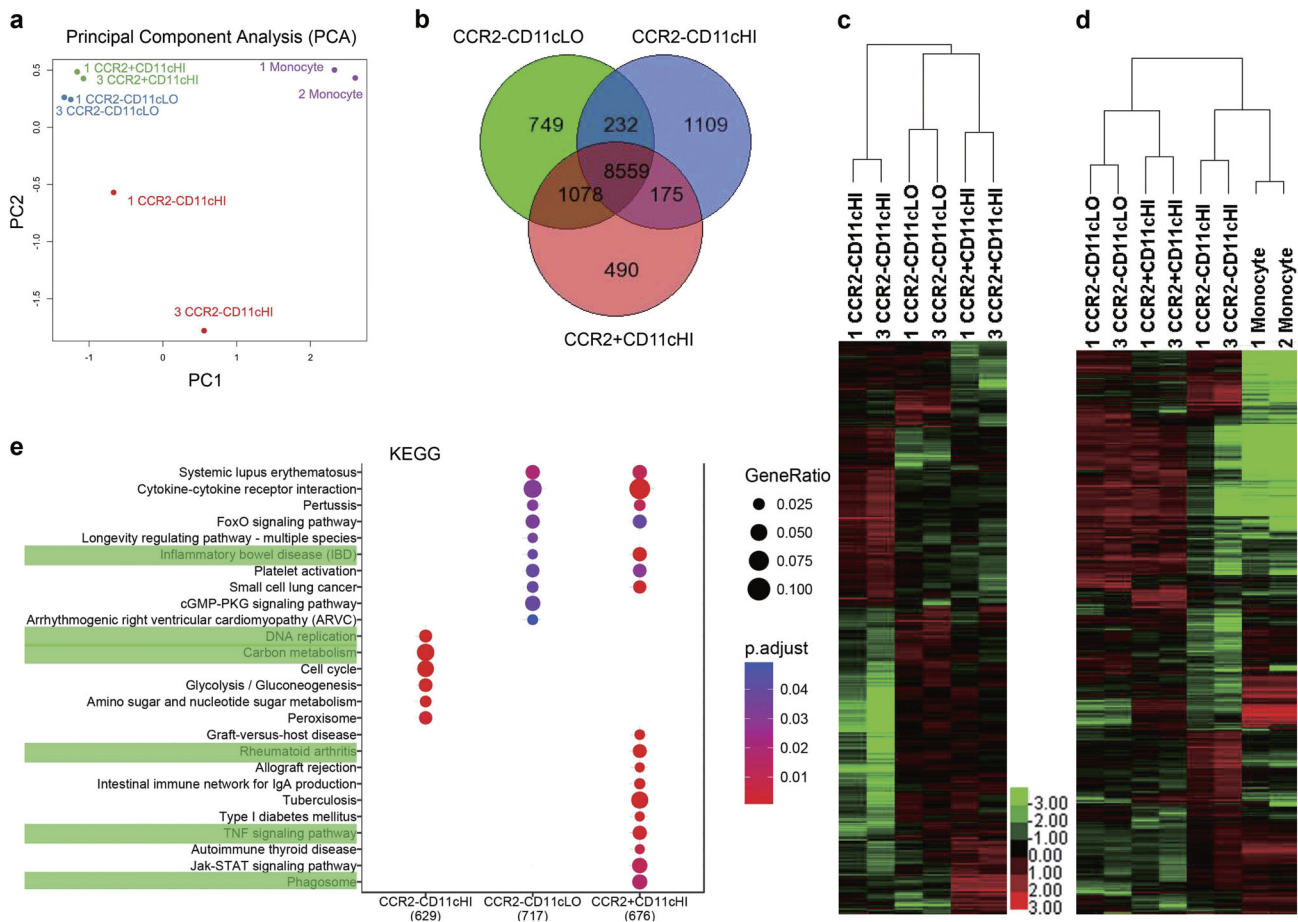


Fig. 3 RNA-Seq analysis of the three decidual macrophage subsets. **a** PCA analysis of the full transcriptome of decidual macrophage subsets and peripheral monocytes. **b** Venn diagram showing 3833 differentially expressed genes between the three macrophage subsets. **c** Heat map of 3833 differentially expressed genes in the three decidual macrophage subsets. **d** Heat map of 3833 differentially expressed genes in the decidual macrophage subsets and peripheral monocytes. **e** Part of the KEGG analysis results based on 3833 differentially expressed genes between the three macrophage subsets

proximal (Fig. 2e) and distal (Fig. 2f) to HLA-G+EVTs and compared the proportion of macrophage subsets. The percentages of CCR2–CD11cHI and CCR2+CD11cHI subsets in macrophages proximal to EVT (Fig. 2g) were significantly higher ($P < 0.001$) than in macrophages distal to EVT (Fig. 2h, i).

Functional denotation of the three decidual macrophage subsets by RNA-Seq analysis

After elucidating the precise localization of the three macrophage subsets at the maternal-fetal interface, we next aimed to explore their functions by analyzing their transcriptional differences. We first performed principle component analysis (PCA) for these three macrophage populations and peripheral monocytes based on the RNA-Seq results (Fig. 3a). The PCA results showed that the transcriptomes of the decidual macrophage subsets were very different from that of peripheral monocytes. Though the CCR2–CD11cLO and CCR2+CD11cHI macrophage subsets expressed different levels of CCR2 and CD11c, their transcriptomes were similar and were significantly different from that of the CCR2–CD11cHI macrophage subset. Next, we sorted out 3833 differentially expressed genes among these three macrophage subsets (Fig. 3b and Supplementary Tables S4 and S5) and clustered them against the three macrophage subsets and monocytes (Fig. 3c, d). Similar to the PCA results, the CCR2–CD11cHI macrophages again showed a marked difference from the other two subsets in the heat map (Fig. 3c), and decidual

macrophage subsets were different from peripheral monocytes (Fig. 3d).

We then performed KEGG and GO-BP enrichment analyses based on the 3833 differentially expressed genes. The KEGG enrichment results showed that the CCR2–CD11cHI macrophages were specifically enriched with cell proliferation and metabolism-related pathways; the CCR2+CD11cHI subset was particularly enriched for tumor necrosis factor (TNF) signaling and phagosome pathways, and few pathways were found to be specifically enriched in the CCR2–CD11cLO subset (Fig. 3e, Supplementary Figure S4a, and Supplementary Table S6). While the CCR2–CD11cLO subset shared many enriched pathways with the CCR2+CD11cHI subset, no overlapping pathways were found between the CCR2–CD11cHI subset and the other two subsets (Fig. 3e and Supplementary Figure S4a). The GO-BP enrichment results were similar to those from the KEGG analysis and again indicated that the CCR2+CD11cHI macrophage population was enriched for certain inflammatory-related items (Supplementary Figure S4b and Supplementary Table S7).

Phagocytic capacity of the three decidual macrophage subsets
Among the phagosome-related genes in the heat map, macrophage receptor with collagenous structure (MARCO) was highly expressed in CCR2+CD11cHI macrophages (Fig. 4a, b). This protein binds Gram-positive and Gram-negative bacteria^{38,39} and enhances the phagocytosis of *C. sordellii*,⁴⁰ a pathogen associated

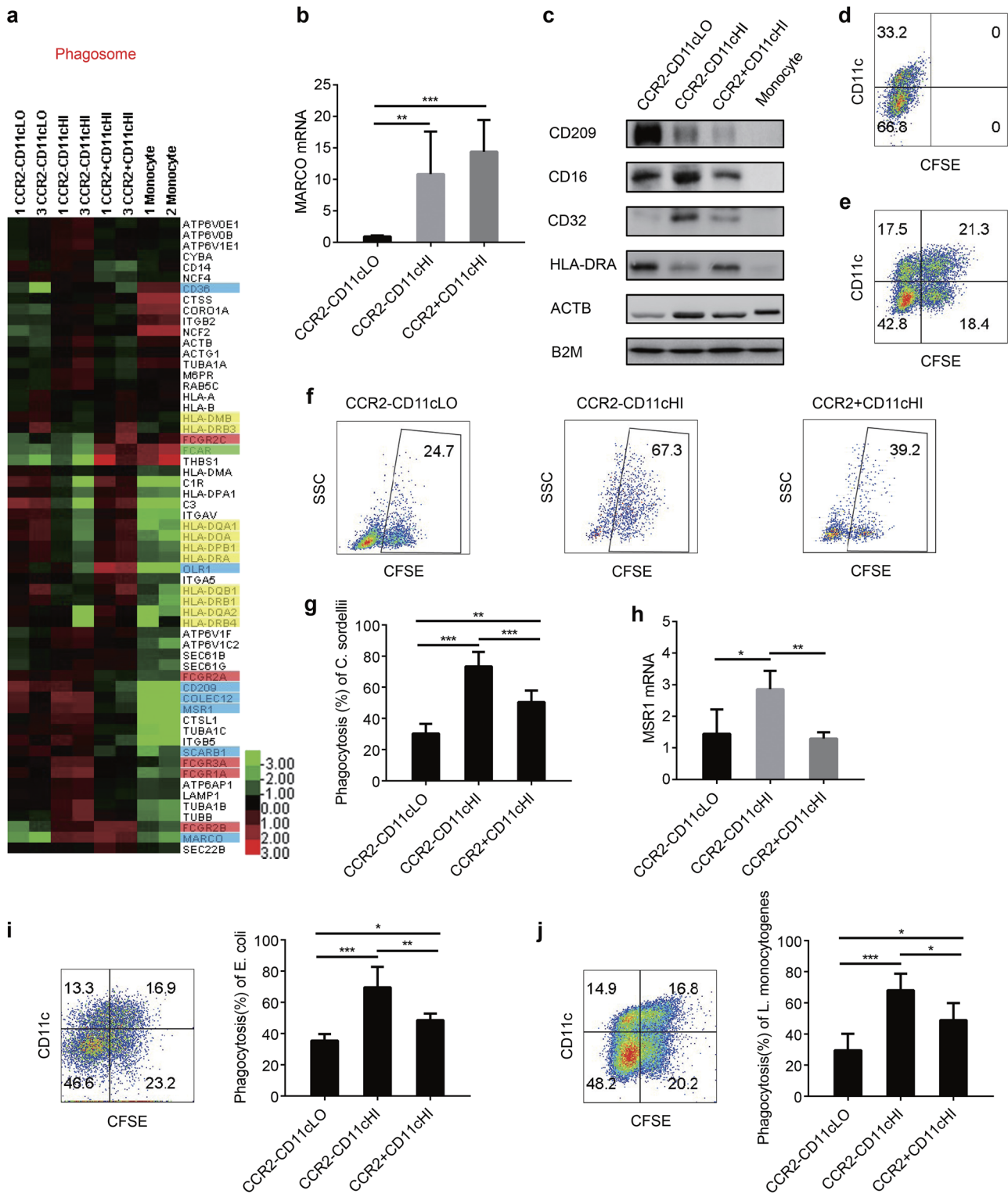


Fig. 4 Phagocytic capacity of the three decidual macrophage subsets. **a** Heat map of highly expressed phagosome-related genes. Red and green: immunoglobulin Fc receptor genes; blue: scavenger receptor genes; yellow: MHCII genes. **b** Real-time PCR results for MARCO in the three decidual macrophage subsets ($n = 6$). **c** Western blot results for phagosome pathway-related proteins. **d** Negative control for the phagocytosis assay. **e** Phagocytosis of *C. sordellii* by total decidual macrophages. **f** Phagocytosis of *C. sordellii* by the three decidual macrophage subsets. **g** The statistical results for the phagocytic capacity of the three macrophage subsets ($n = 6$). **h** Real-time PCR results for MSR1 in the three decidual macrophage subsets ($n = 6$). **i** Phagocytosis of *E. coli* by total decidual macrophages, and the statistical results for the phagocytic capacity of the three macrophage subsets ($n = 6$). **j** Phagocytosis of *L. monocytogenes* by total decidual macrophages, and the statistical results for the phagocytic capacity of the three macrophage subsets ($n = 6$). **b, g–j** One-way ANOVA, $***P < 0.001$

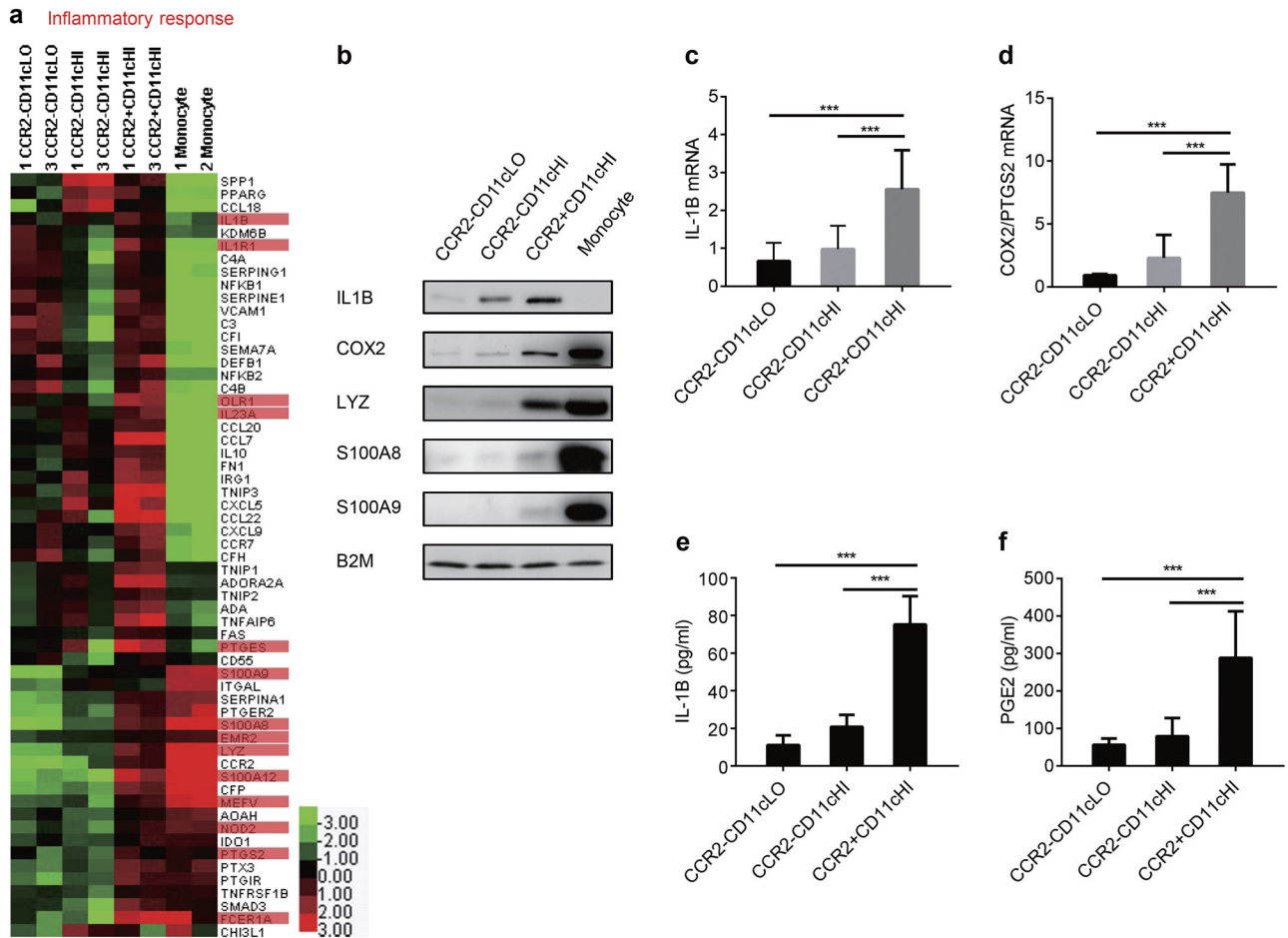


Fig. 5 CCR2+CD11cHI macrophages are pro-inflammatory. **a** Heat map of inflammatory response-related genes based on GO-BP analysis. Red: pro-inflammatory genes. **b** Western blot results for pro-inflammatory genes in the three decidual macrophage subsets and monocytes. **c**, **d** Real-time PCR results for IL1B and COX2 in the three decidual macrophage subsets ($n = 6$). **e**, **f** ELISA results for IL1B and PGE2 in the supernatants of the three decidual macrophage subsets ($n = 6$). **c–f** One-way ANOVA, $***P < 0.001$

with highly lethal female reproductive tract infections.⁴¹ MARCO-deficient mice have a high rate of death when infected by intrauterine injection with *C. sordellii*.⁴⁰ The high expression levels of MARCO and other phagosome-related genes, such as immunoglobulin alpha Fc receptor (FCAR), oxidized low-density lipoprotein receptor 1 (OLR1) and major histocompatibility complex II (MHCII) members, including HLA class II histocompatibility antigen and DR alpha chain (HLA-DRA) in CCR2+CD11cHI macrophages (Fig. 4a–c), suggested that this subset was highly phagocytic. To test this hypothesis, we performed a phagocytosis experiment (Fig. 4d, e), and the CCR2+CD11cHI macrophages showed more enhanced phagocytosis of *C. sordellii* than the CCR2–CD11cLO macrophages ($P < 0.01$, Fig. 4f, g). Surprisingly, the CCR2–CD11cHI macrophages phagocytosed *C. sordellii* even more effectively than the CCR2+CD11cHI macrophages ($P < 0.001$, Fig. 4f, g). The reason for this phenomenon might be that CCR2–CD11cHI macrophages not only expressed high levels of MARCO and macrophage scavenger receptor types I and II (MSR1, Fig. 4a, h), but also other phagosome-related genes, such as beta-actin (ACTB), platelet glycoprotein 4 (CD36), and the immunoglobulin gamma Fc receptors CD16 and CD32 (Fig. 4a, c). Although the phagocytic capacity of the CCR2–CD11cLO macrophages was the lowest, these cells still expressed high levels of some phagocytic genes, including CD209 (Fig. 4a, c). We also examined the phagocytosis of *E. coli* and *L. monocytogenes* by these three decidual macrophage subsets and obtained similar results (Fig. 4,

j). Together, these results suggest that the CCR2–CD11cHI and CCR2+CD11cHI macrophages can effectively clear many types of potential invading pathogens around EVT, thus maintaining a healthy pregnancy.

CCR2+CD11cHI macrophages are pro-inflammatory, while CCR2–CD11cHI macrophages are anti-inflammatory
To confirm the pro-inflammatory characteristics of the CCR2+CD11cHI macrophages as indicated by GO-BP enrichment analysis, we compared the expression of the identified inflammatory response-related genes in the heat map (Fig. 5a). Both the pro-inflammatory genes interleukin-1 beta (IL1B) and prostaglandin G/H synthase 2 (PTGS2/COX2) were highly expressed in the CCR2+CD11cHI macrophages, as also shown by western blot and real-time PCR analyses (Fig. 5b–d). Furthermore, the levels of the secreted forms of IL1B (Fig. 5e) and PGE2 (Fig. 5f), which are produced by COX2, were also the highest in the CCR2+CD11cHI macrophages ($P < 0.001$) based on ELISA. Lysozyme C (LYZ) was also found to be highly expressed in the CCR2+CD11cHI macrophages (Fig. 5a, b), and LYZ may help this subset to directly lyse bacteria.⁴² These results suggested that the CCR2+CD11cHI macrophages proximal to EVT may be involved in establishing a pro-inflammatory milieu at the maternal-fetal interface, thus assisting in the defense and clearance of invading pathogens.

The CCR2–CD11cHI macrophages expressed higher levels of carbon metabolism genes. We verified this finding by performing

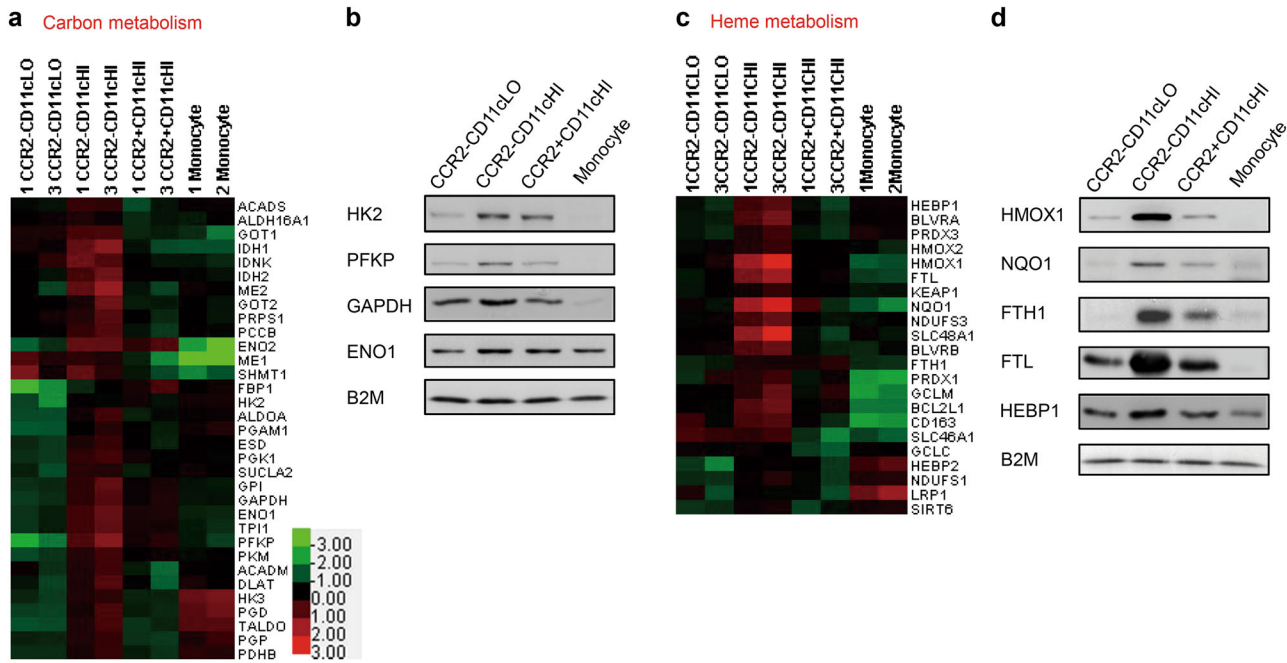


Fig. 6 CCR2–CD11cHI macrophages expressed the highest levels of heme metabolism-related genes. **a** Heat map of carbon metabolism-related genes based on the KEGG results. **b** Western blot results for carbon metabolism-related proteins. **c** Heat map of reported heme metabolism-related genes in decidual macrophage subsets and monocytes. **d** Western blot results for critical heme metabolism-related proteins

western blot analysis with hexokinase-2 (HK2), alpha-enolase (ENO1), and glyceraldehyde-3-phosphate dehydrogenase (GAPDH) antibodies (Fig. 6a, b). To further elucidate the function of this subset, we examined all of the specifically expressed genes in the CCR2–CD11cHI macrophages and found that these cells also showed much higher expression of genes involved in heme metabolism (Fig. 6c). Almost all of the critical heme metabolism-related genes⁴³ were highly expressed in the CCR2–CD11cHI macrophages, including ferritin heavy chain (FTH1), NAD(P)H: quinone oxidoreductase 1 (NQO1), and HMOX1 (Fig. 6d). Inducible HMOX1 can catabolize toxic-free heme into equimolar amounts of Fe²⁺, carbon monoxide, and biliverdin.⁴³ The HMOX1 molecule has been convincingly confirmed to be anti-oxidative and anti-inflammatory and thus to act in a cytoprotective manner.^{43,44} Carbon monoxide and bilirubin, which are produced by heme metabolism, are also antioxidants.⁴³ Therefore, the CCR2–CD11cHI macrophages may play an anti-inflammatory role during early pregnancy.

DISCUSSION

In this study, we reported that there are three macrophage subsets with different functions at the maternal-fetal interface (Fig. 7). They are CCR2–CD11cHI, CCR2+CD11cHI, and CCR2–CD11cLO. The CCR2–CD11cHI and CCR2+CD11cHI subsets exhibit a polar distribution at the maternal–fetal interface, while the third subset (CCR2–CD11cLO) is widely distributed; functionally, these three decidual macrophage subsets all show phagocytic capacity, though at different levels, and the CCR2–CD11cHI and CCR2+CD11cHI macrophages maintain an inflammatory balance at the maternal–fetal interface (Fig. 7). To our knowledge, this is the first report of three decidual macrophage subsets during early human pregnancy. Furthermore, this study also provides further evidence that tissue-resident macrophages have subsets following the identification of three lung interstitial macrophage subsets based on the expression of CD11c and MHCII in mice.⁴⁵

The CCR2–CD11cLO subset comprises the majority of macrophages, and they are extensively present in the decidua, particularly in the decidua parietalis, where there are no EVT. These macrophages exhibit the fewest inflammatory properties and appear to be in a static state. However, they highly express CD209 and MHCII (Fig. 4a, c), so they may play a role in antigen presentation at the maternal–fetal interface. Regarding why the CD11cHI macrophage subsets exhibit a polar distribution and specifically reside proximal to EVTs, we considered that the CCR2–CD11cHI macrophages may be induced or recruited by free heme released by the stress response at the maternal–fetal interface.⁴³ The CCR2+CD11cHI subset may be recruited toward EVTs by excessive chemotactic CCL2 produced by the pro-inflammatory micro niche created by the interaction between EVTs and decidual stromal cells.⁴⁶ However, the precise mechanism requires further investigation.

The CCR2–CD11cHI decidual macrophages specifically expressed HMOX1 and comprised ~5% of the decidual macrophages. The identification of this minority macrophage population is remarkable. Female *Hmox1*^{-/-} mice were infertile.^{43,47} Breeding *Hmox1*^{-/+} mice only gave birth to 1–8% viable *Hmox1*^{-/-} progeny depending on the genetic background, suggesting that HMOX1 plays crucial roles during pregnancy and that abnormal expression of this molecule results in adverse pregnancy outcomes.⁴⁷ The existence of cytoprotective HMOX1+ decidual macrophages, which are localized adjacent to EVTs, may help to protect the fetus from being affected by possible infections during early stages of gestation. Subsequent studies should concentrate on the function of HMOX1 in the CCR2–CD11cHI macrophages and its relationship with physiological or pathological pregnancy outcomes.

Overall, we confirmed the existence of three distinct macrophage subsets and explored their functions at the maternal–fetal interface. We believe that this study starts to unveil the complicated maternal–fetal crosstalk that occurs during early human pregnancy.

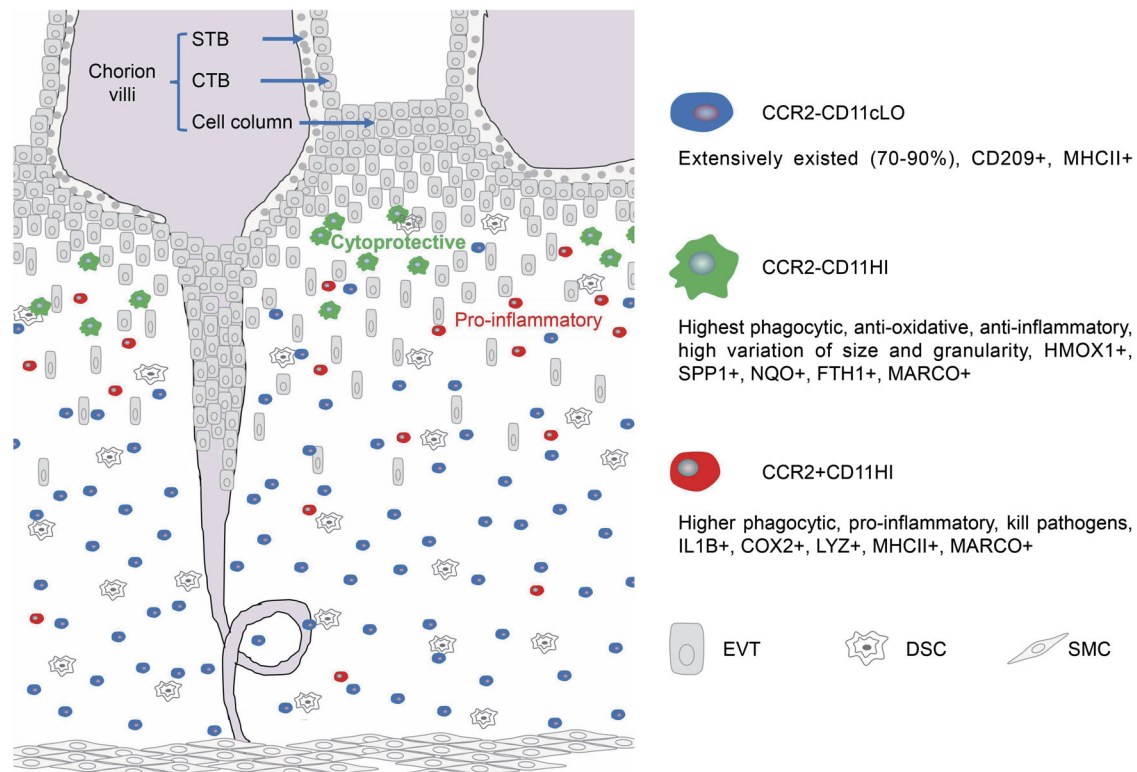


Fig. 7 A proposed model for the distribution and major functions of the three macrophage subsets at the maternal–fetal interface during early human pregnancy. The widely distributed CCR2–CD11cLO macrophages highly express CD209 and MHCII, so they may play a role in antigen presentation at the maternal–fetal interface. CCR2+CD11cHI macrophages, which are mainly proximal to EVTs, secrete high levels of IL1B and PGE2 and thus have the ability to create a pro-inflammatory microenvironment to help combat possible invading uterine pathogens. CCR2–CD11cHI macrophages, which are primarily proximal to EVTs, show the highest phagocytic capacity and metabolic activity. Almost all of the critical heme metabolism-related genes are highly expressed in CCR2–CD11cHI macrophages, so these macrophages may help to clear heme and serve as a brake for excess inflammation, thus conferring protection and establishing an inflammatory balance with CCR2+CD11cHI macrophages around EVTs. EVT extravillous trophoblast cell, DSC decidual stromal cell, SMC smooth muscular cell, STB syncytiotrophoblast, CTB cytotrophoblast cell

ACKNOWLEDGEMENTS

We thank Xili Zhu and Shiwen Li for confocal image capture, Hua Qin for FACS, Can Peng and Lei Sun for TEM, and Tingting Wu for the phagocytosis experiment. We thank Meijing Wang, Rong Jing, and Jinglei Zhai for collecting samples from the hospital, and we thank Yong Zhao, Jingpian Peng, Yanling Wang, and Jay. C. Cross for discussion. This study was supported by grants from the National Natural Science Foundation of China (81490741 and 81401224) and the Ministry of Science and Technology of the People's Republic of China (2016YFC1000208 and 2017YFC1001401).

AUTHORS' CONTRIBUTIONS

X.J. performed the experiments. H.W. and X.J. designed the study and interpreted the data. M.L. collected samples from the hospital. X.J. wrote the original manuscript. M.R. D. and H.W. modified the manuscript.

ADDITIONAL INFORMATION

Supplementary information accompanies this paper at (<https://doi.org/10.1038/s41423-018-0008-0>).

Competing interests: The authors declare no competing interests.

REFERENCES

1. Erlebacher, A. Immunology of the maternal-fetal interface. *Annu. Rev. Immunol.* **31**, 387–411 (2013).
2. Wallace, A. E., Whitley, G. S., Thilaganathan, B. & Cartwright, J. E. Decidual natural killer cell receptor expression is altered in pregnancies with impaired

vascular remodeling and a higher risk of pre-eclampsia. *J. Leukoc. Biol.* **97**, 79–86 (2015).

3. Fu, B. et al. Natural killer cells promote fetal development through the secretion of growth-promoting factors. *Immunity* **47**, 1100–1113 (2017). e1106.
4. Zhang, J. et al. Human dNK cell function is differentially regulated by extrinsic cellular engagement and intrinsic activating receptors in first and second trimester pregnancy. *Cell. Mol. Immunol.* **14**, 203–213 (2017).
5. Aluvihare, V. R., Kallikourdis, M. & Betz, A. G. Regulatory T cells mediate maternal tolerance to the fetus. *Nat. Immunol.* **5**, 266–271 (2004).
6. Lash, G. E. et al. Decidual macrophages: key regulators of vascular remodeling in human pregnancy. *J. Leukoc. Biol.* **100**, 315–325 (2016).
7. Abrahams, V. M., Kim, Y. M., Straszewski, S. L., Romero, R. & Mor, G. Macrophages and apoptotic cell clearance during pregnancy. *Am. J. Reprod. Immunol.* **51**, 275–282 (2004).
8. Egashira, M. et al. F4/80+ macrophages contribute to clearance of senescent cells in the mouse postpartum uterus. *Endocrinology* **158**, 2344–2353 (2017).
9. Hamilton, S. et al. Macrophages infiltrate the human and rat decidua during term and preterm labor: evidence that decidual inflammation precedes labor. *Biol. Reprod.* **86**, 39 (2012).
10. Wang, H. et al. Role of decidual CD14(+) macrophages in the homeostasis of maternal-fetal interface and the differentiation capacity of the cells during pregnancy and parturition. *Placenta* **38**, 76–83 (2016).
11. Care, A. S. et al. Macrophages regulate corpus luteum development during embryo implantation in mice. *J. Clin. Invest.* **123**, 3472–3487 (2013).
12. Murray, P. J. et al. Macrophage activation and polarization: nomenclature and experimental guidelines. *Immunity* **41**, 14–20 (2014).
13. Gustafsson, C. et al. Gene expression profiling of human decidual macrophages: evidence for immunosuppressive phenotype. *PLoS ONE* **3**, e2078 (2008).
14. Jaiswal, M. K. et al. V-ATPase upregulation during early pregnancy: a possible link to establishment of an inflammatory response during preimplantation period of pregnancy. *Reproduction* **143**, 713–725 (2012).

15. Zhang, Y. H., He, M., Wang, Y. & Liao, A. H. Modulators of the balance between M1 and M2 macrophages during pregnancy. *Front. Immunol.* **8**, 120 (2017).
16. Ning, F., Liu, H. & Lash, G. E. The role of decidual macrophages during normal and pathological pregnancy. *Am. J. Reprod. Immunol.* **75**, 298–309 (2016).
17. Heyward, C. Y. et al. The decidua of preeclamptic-like BPH/5 mice exhibits an exaggerated inflammatory response during early pregnancy. *J. Reprod. Immunol.* **120**, 27–33 (2017).
18. Tsao, F. Y., Wu, M. Y., Chang, Y. L., Wu, C. T., Ho, H. N. M1 macrophages decrease in the deciduae from normal pregnancies but not from spontaneous abortions or unexplained recurrent spontaneous abortions. *J. Formos. Med. Assoc.* (2017).
19. Xu, Y. et al. An M1-like macrophage polarization in decidual tissue during spontaneous preterm labor that is attenuated by rosiglitazone treatment. *J. Immunol.* **196**, 2476–2491 (2016).
20. Gomez-Lopez, N., StLouis, D., Lehr, M. A., Sanchez-Rodriguez, E. N. & Arenas-Hernandez, M. Immune cells in term and preterm labor. *Cell. Mol. Immunol.* **11**, 571–581 (2014).
21. Fu, B. et al. CD11b and CD27 reflect distinct population and functional specialization in human natural killer cells. *Immunology* **133**, 350–359 (2011).
22. Zeng, W. et al. Distinct transcriptional and alternative splicing signatures of decidual CD4+ T cells in early human pregnancy. *Front. Immunol.* **8**, 682 (2017).
23. Piccinni, M. P. et al. Defective production of both leukemia inhibitory factor and type 2 T-helper cytokines by decidual T cells in unexplained recurrent abortions. *Nat. Med.* **4**, 1020–1024 (1998).
24. Houser, B. L., Tilburgs, T., Hill, J., Nicotra, M. L. & Strominger, J. L. Two unique human decidual macrophage populations. *J. Immunol.* **186**, 2633–2642 (2011).
25. Tilburgs, T. et al. Human HLA-G+ extravillous trophoblasts: Immune-activating cells that interact with decidual leukocytes. *Proc. Natl Acad. Sci. USA* **112**, 7219–7224 (2015).
26. Li, Y. H. et al. The Galectin-9/Tim-3 pathway is involved in the regulation of NK cell function at the maternal-fetal interface in early pregnancy. *Cell. Mol. Immunol.* **13**, 73–81 (2016).
27. Hung, J. H. & Weng, Z. Analyzing MicroarrayData. *Cold Spring Harb. Protoc.* **2017**, pdbprot093112 (2017).
28. Law, C. W., Alhamdoosh, M., Su, S., Smyth, G. K. & Ritchie, M. E. RNA-seq analysis is easy as 1-2-3 with limma, Glimma and edgeR. *F1000Res* **5**, 1408 (2016).
29. Kanehisa, M., Sato, Y., Kawashima, M., Furumichi, M. & Tanabe, M. KEGG as a reference resource for gene and protein annotation. *Nucleic Acids Res.* **44**, D457–D462 (2016).
30. Rhee, S. Y., Wood, V., Dolinski, K. & Draghici, S. Use and misuse of the gene ontology annotations. *Nat. Rev. Genet.* **9**, 509–515 (2008).
31. Yu, G., Wang, L. G., Han, Y. & He, Q. Y. clusterProfiler: an R package for comparing biological themes among gene clusters. *OMICS* **16**, 284–287 (2012).
32. Pirooznia, M., Nagarajan, V. & Deng, Y. GeneVenn - a web application for comparing gene lists using Venn diagrams. *Bioinformatics* **1**, 420–422 (2007).
33. Wang, Z. et al. Interferon-gamma inhibits nonopsonized phagocytosis of macrophages via an mTORC1-c/EBPbeta pathway. *J. Innate Immun.* **7**, 165–176 (2015).
34. Kurihara, T., Warr, G., Loy, J. & Bravo, R. Defects in macrophage recruitment and host defense in mice lacking the CCR2 chemokine receptor. *J. Exp. Med.* **186**, 1757–1762 (1997).
35. Zheng, Y. et al. Structure of CC chemokine receptor 2 with orthosteric and allosteric antagonists. *Nature* **540**, 458–461 (2016).
36. Zhang, Y. et al. Human trophoblast cells induced MDSCs from peripheral blood CD14(+) myelomonocytic cells via elevated levels of CCL2. *Cell. Mol. Immunol.* **13**, 615–627 (2016).
37. Guilliams, M. & Scott, C. L. Does niche competition determine the origin of tissue-resident macrophages? *Nat. Rev. Immunol.* **17**, 451–460 (2017).
38. Elomaa, O. et al. Structure of the human macrophage MARCO receptor and characterization of its bacteria-binding region. *J. Biol. Chem.* **273**, 4530–4538 (1998).
39. Arredouani, M. et al. The scavenger receptor MARCO is required for lung defense against pneumococcal pneumonia and inhaled particles. *J. Exp. Med.* **200**, 267–272 (2004).
40. Thelen, T. et al. The class A scavenger receptor, macrophage receptor with collagenous structure, is the major phagocytic receptor for *Clostridium sordellii* expressed by human decidual macrophages. *J. Immunol.* **185**, 4328–4335 (2010).
41. Aldape, M. J., Bryant, A. E. & Stevens, D. L. *Clostridium sordellii* infection: epidemiology, clinical findings, and current perspectives on diagnosis and treatment. *Clin. Infect. Dis.* **43**, 1436–1446 (2006).
42. Callewaert, L. & Michiels, C. W. Lysozymes in the animal kingdom. *J. Biosci.* **35**, 127–160 (2010).
43. Gozzelino, R., Jeney, V. & Soares, M. P. Mechanisms of cell protection by heme oxygenase-1. *Annu. Rev. Pharmacol. Toxicol.* **50**, 323–354 (2010).
44. Naito, Y., Takagi, T. & Higashimura, Y. Heme oxygenase-1 and anti-inflammatory M2 macrophages. *Arch. Biochem. Biophys.* **564**, 83–88 (2014).
45. Gibbings, S. L. et al. Three unique interstitial macrophages in the murine lung at steady state. *Am. J. Respir. Cell Mol. Biol.* **57**, 66–76 (2017).
46. Hess, A. P. et al. Decidual stromal cell response to paracrine signals from the trophoblast: amplification of immune and angiogenic modulators. *Biol. Reprod.* **76**, 102–117 (2007).
47. Ozen, M., Zhao, H., Lewis, D. B., Wong, R. J. & Stevenson, D. K. Heme oxygenase and the immune system in normal and pathological pregnancies. *Front. Pharmacol.* **6**, 84 (2015).